Nonlinear State-Space Projection Based Method to Acquire EEG and ECG Components Using a Single Electrode

Motoki Sakai[1], Yuichi Okuyama[2], Toshihiro Sato[3], Daming Wei[4]

[1]Graduate School of Symbiotic System Science and Technology, Fukushima University, Kanayagawa, Fukushima City, Fukushima 960-1296, Japan

[2]Division of Computer Engineering, University of Aizu, Aizu-Wakamatsu City, Fukushima, 965-8580 Japan

[3]Graduate School of Computer Science and Engineering, University of Aizu, Aizu-Wakamatsu City, Fukushima, 965-8580 Japan

[4]Graduate School of Medicine, Tohoku University, 2-1 Seiryo-machi, Aoba-ku, Sendai, Miyagi, 980-8575, Japan

[1]m.sakai510@gmail.com; [4]daming.wei@bme-lab.biz

Abstract- **In some diagnoses, such as the polysomnography, simultaneous measurement of the electroencephalogram (EEG) and the electrocardiogram (ECG) is often required. It would be more efficient if both the EEG and ECG could be obtained simultaneously by using a single measurement. In this paper, we introduce a nonlinear state-space projection-based technique to extract the EEG and ECG components from an EEG signal measured with a non-cephalic reference (NCR) that guarantees accurate detection of R waves in the EEG measurement. Evaluation of the method using simulated data showed that the improved normalized power spectrum in alpha, beta (13–30 Hz), and theta bands were accurate. In an accrual EEG, measured using the NCR electrode, it was confirmed that the frequency components of the extracted EEG were accurate, and no spikes that could be attributed to the ECG component were observed in the resultant EEG signal.**

Keywords- Polysomnography; EEG; ECG; Non-Cephalic Reference; Nonliner State-Space Projection

I INTRODUCTION

The electroencephalogram (EEG) and the electrocardiogram (ECG) are frequently measured in some diagnostic procedures such as the polysomnography or the hybrid brain-computer interface (BCI). In addition, they are used in ambulatory monitoring [1,2]. However, multichannel recording can be inconvenient and can often cause stress to the patient even though EEG and ECG which are effective for monitoring the physiological signals of human beings. Therefore, it is desirable to simultaneously record EEG and ECG signals using a single electrode. We propose a method to simultaneously obtain both EEG and ECG signals using a single active electrode and a non-cephalic referential electrode.

A standard EEG signal is usually measured with an ear reference. In some rare cases, the ECG components, which are regarded as artifacts to be removed, can be observed in the EEG signal, although the EEG recording does not always acquire the ECG component [1]. In our previous work [4, 5, 6], we attempted to move the reference electrode used for the EEG recording from the ear to a non-cephalic location in order to more reliably obtain ECG components in EEG measurements; this reference electrode was described as a non-cephalic reference (NCR) electrode. The ECG components measured with the NCR electrode were sufficiently strong as compared to the EEG components to allow for further processing. We found that EEG and ECG components could be obtained in a single measurement if an EEG-ECG combined signal from the NCR electrode is separated into two components by using an appropriate method. Our current objective is to develop a signal processing algorithm that can separate the EEG and ECG signals to extract EEG components in the frequency domain and detect peaks of the R wave of the ECG for a heart rate analysis.

To separate the EEG-ECG combined signal, we proposed three methods in our previous studies [4, 5, 6]. The first was based on signal averaging ECG (SAECG) and wavelet transformation [5]. Generally, the SAECG method is used to remove ECG artifacts from the EEG signal (however, in our study, the ECG component was not treated as an artifact to be eliminated). Nevertheless, the resultant signal contains some non-negligible residual ECG components, which have harmful effects in terms of EEG frequency analysis. In our research [5], wavelet transformation was used to remove residual components attributed to the SAECG, and most frequency components of EEG were extracted from EEG-ECG combined signal measured with the NCR electrode. The other two methods were realized in the opposite manner as the first method; regarding the ECG as the major signal and the EEG as a type of EMG-like noise, where the EEG signal was first removed to obtain an estimated ECG from the raw signal. In [5], the combined EEG-ECG signal was decomposed by five scale levels and the wavelet shrinkage, a technique to eliminate noise from the ECG, was performed to separate EEG components from the combined EEG-ECG signal. Because the shrinkage function was ineffective for approximation level five, we proposed a processing method based on cosine window function. A combination of wavelet shrinkage and the cosine window function could separate the EEG and ECG components from the mixed signal, implying that denoising algorithms for the ECG signal can be applied to separate EEG and ECG components. In [6], the application of the cosine window function proposed in [4] was improved. In [4], in approximation level five, the wavelet coefficient was determined using a window function of a fixed size. However, given the fluctuations of ECG durations, a variable window size is preferable, and thus, a variable window operation was proposed. Although the shape of the separated ECG components was rough, this method was shown to separate EEG and ECG signals that included ectopic beats, which was a significant feature among the three methods because the SAECG-based method[5] could not distinguish ectopic beats.

In the above-described methods [4-6], estimation of EEG and ECG components depended on the periodicity of the ECG component. These processes were not suitable when the separated EEG and ECG components had to be applied on a real-time basis, such as in the hybrid BCI [11], because the analysis of the EEG signal must be controlled by the periodicity of the ECG component. Therefore, a method that is not regulated by the periodicity of the ECG component would be more effective for a real-time EEG-based analysis. In this paper, we propose a suitable algorithm to accomplish this objective.

In a previous study [7], five denoising methods were compared for the single electrode ECG, and nonlinear state-space projection [8, 9] was found to be the most effective. Nonlinear state-space projection is based on the principle component analysis of the phase space of a dynamical system. While the methods [4-6] explored in our previous studies were dependent on the periodicity of the ECG component, nonlinear state-space projection can be performed on every sample. However, limitations of nonlinear state-space projection include the requirement of a computationally intensive high-dimensional nearest neighbor search, although it can be expected to estimate a clearly shaped ECG. Although nonlinear state-space projection has advantages as well as disadvantages, it produces a superior performance in terms of SNR. In addition, it offers the potential to obtain a clear EEG component independent of the periodicity of the ECG component. In this paper, we evaluate the feasibility of nonlinear state-space projection as a method of separating the EEG and ECG components from a single measurement.

II METHOD

A. Nonlinear State-Space Projection

Nonlinear state-space projection is a technique [8, 9] that can be used to separate the ECG signal from other components, e.g., artifacts and noise. Particularly, in [9], this technique was used similarly to our proposed application to extract a fetal ECG from the maternal ECG. In [9], an accurate fetal ECG needed to be extracted to perform a diagnostic technique for fetal cardiac activity. This study appears similar to our study, in that both the ECG and the separated component need to be made available in these studies.

The first step of a general nonlinear method is to reconstruct the phase space of the dynamical system, for example, by using delay coordinates $X_n = (x_{n-m+1} \cdots, x_n)$. Fig. 1 shows the two-dimensional delay representation; the one on the left was generated from a clean ECG signal, while the one on the right was extracted from a noisy ECG. It is intuitively understood that nonlinear state-space projection predicts the clean delay representation on the left from the noisy one on the right. Xn is defined as an embedded vector and is equivalent to the true dynamic coordinates, provided the embedding dimension m is sufficiently large. Herein, approximate projections are used locally in the reconstructed phase space to separate the EEG components from the combined EEG-ECG signal.

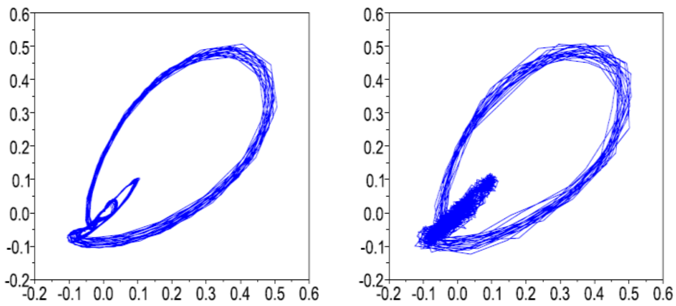

Fig. 1 Delay representation of ECG signals (Left: clean ECG, Right: noisy ECG)

A procedure to compute the correction for the nth embedding vector (yn = the embedded vector of the EEG-ECG combined signal) constitutes the following eight steps.

1) The delay coordinates yn are generated. The embedding dimension (m) is set to 200 (m was selected empirically).

2) A small neighborhood (u) around the point (n) is searched. The index for the set of points falling in this neighborhood is denoted as un, and hence, the neighboring points are designated as $y_j, j \in u_n$, where $|u_n|$ is the total number of points in the neighborhood. In the following example, the neighborhood size was set to the smallest value that produced k_m neighbors, with no less than 50 units. From the points $y_k, k \in u_n$, we constructed the mean

$$\eta_i = \frac{1}{|u_n|}\sum_{k \in u_n} y_{k-m+i} \qquad i = 1, \cdots m \tag{1}$$

3) In an embedding space with dimension m, the covariance matrix of all delay vectors is computed in a small neighborhood surrounding a given point, which should be corrected

$$C_{ij} = \frac{1}{|u_n|}\sum_{k \in u_n} y_{k-m+i} y_{k-m+j} - \eta_i \eta_j \tag{2}$$

4) The eigenvectors and the eigenvalues of this matrix are calculated under the assumption that the clean signal exists near a smooth manifold with dimension d < m, and that the variance of the EEG is smaller than that of the ECG signal.

5) Large eigenvalues correspond to the directions for the signal, and small ones correspond to all other directions. Therefore, the vector under consideration is moved towards the subspace of large eigenvectors to separate the EEG signal.

6) To penalize corrections based on the first and last coordinates in the delay window, the equation $R_{11} = R_{mm} = r$ is applied, where r is a large value. Other values along the diagonal of R are set to one. The Q orthogonal eigenvectors of the covariance matrix with the smallest eigenvalues are called $e_q, q = 1, \cdots Q$. The projector onto the subspace spanned by these vectors is then

$$Q_{ij} = \sum_{q=1}^{Q} e_{q,i} e_{q,j} \tag{3}$$

7) The ith component of the correction θ_n is given by

$$\theta_{n,i} = \frac{1}{R_{ii}} \sum_{j=0}^{m} Q_{ij} R_{jj} (\eta_j - y_{n-m+j}) \quad (4)$$

8) Finally, the correction θ_n is added to each original embedded vector to bring the point towards the manifold spanned by the m-Q largest eigenvectors. Then, an estimated embedded vector of the ECG component is obtained. Note that the R penalty matrix yields the two largest eigenvalues, which lie in the subspace spanned by the first and last coordinates of the embedding space, and prevents the correction vector from having any components in the these directions.

These steps are performed for each embedding vector. Given that each element of the scalar time series occurs in m different embedding vectors, many different suggested corrections are obtained. In our study, one of the suggestions was selected for further evaluation.

B. R Wave Detection Method: Smoothing Nonlinear Energy Operator

In our previous research [4-6], a smoothing nonlinear energy operator (SNEO) was applied to detect the R-wave peaks in the EEG signal [10]. The SNEO is sensitive to instantaneous changes in frequency-dependent energy and can emphasize R-waves that corrupt the EEG signal by the Teager-Kaiser energy operator [10].

III EVALUATIONS AND RESULTS

The proposed method was evaluated using both simulated and actual data measurements recorded using a NCR electrode.

A. Evaluation Using Simulated Data

We simulated the target signal by blending the actual, measured lead I ECG and O2-lead EEG signals recorded from four subjects, including three males and one female, all aged 21 to 22 years. The duration of each EEG measurement is approximately five minutes. The sampling rate of both the measurements was 250 Hz, and both were filtered using a 0.5–40 Hz band-pass filter. The EEG and the ECG data for each subject were combined with several ratios of the EEG and ECG to generate the simulated data. Eq. (5) defines the ratio between the EEG and ECG components, which is called the spike-to-background signal energy ratio (SBR) [9].

$$SBR = \frac{(1/N_k)\sum_{k=1}^{N_k}((1/N_S^{(k)})\sum_{n=1}^{N_S^{(k)}} SE^{(k)}(n))}{(1/N_B)\sum_{n=1}^{N_B} EE(n)} \quad (5)$$

$SE^{(k)}(n)$ is the energy of the kth QRS complex with $N_S^{(k)}$ points, N_k is the number of spikes in the entire signal, and EE(n) is the energy of the EEG signal in the nonspiked area with N_B points.

A value of m = 200 was set for the embedded space to generate the delay coordinates, and then, nonlinear state-space projection was performed to separate the signals. To evaluate the separated EEG component, the improved normalized power spectrum (INPS) was calculated for the delta, theta, alpha, and beta (beta1:13–30 Hz and beta2: 30–40 Hz) components, respectively.

In Eq. (6), P is the power spectrum of the EEG signals calculated by using FFT, and the summation is carried for the corresponding frequency band. The closer the INPS is to 1, the more accurate is the result.

$$INPS = \frac{\sum P_{EEG}}{\sum P_{EstimatedEEG}} \quad (6)$$

Figs. 2(a), (b), (c), (d), and (e) show the original EEG, ECG, simulated EEG-ECG combined signal, estimated ECG, and estimated EEG signal, respectively. Fig. 3 shows INPS, where the SBRs were 10, 50, and 90. Fig. 3(a)–(e) shows the INPS of the alpha, beta1, beta2, delta, and theta bands, respectively. In Fig. 2, ns = 10, ns = 25, and ns = 50 indicate the neighborhood size. In this evaluation, the estimated EEG components were reconstructed with Q = 2, as discussed below.

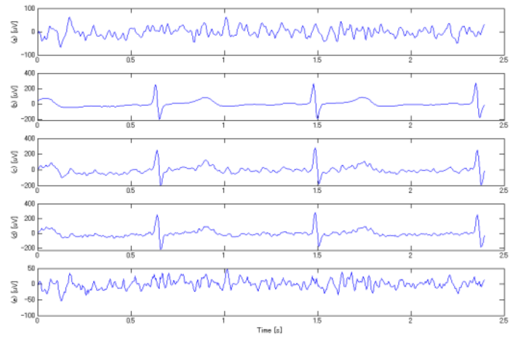

Fig. 2 (a) Original EEG, (b) original ECG, (c) simulated signal, (d) estimated ECG signal, (e) estimated EEG signal

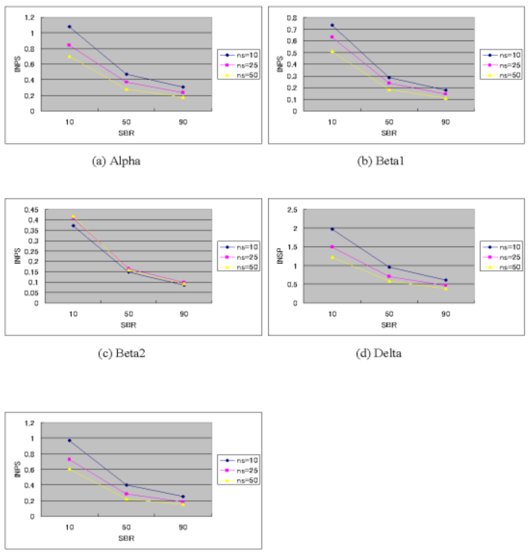

(a) Alpha (b) Beta1 (c) Beta2 (d) Delta (e) Theta

Fig. 3 Results of the *INPS* from the simulation data; (a)–(e) are the results of the *INPS* from the alpha, beta1, beta2, delta, and theta bands, respectively

B. Evaluation of signals recorded using an NCR electrode

Examples of actual signals recorded using the NCR electrode are shown in Figs. 4 and 5. The EEG electrode is located at lead O2, and the NCR electrode is located at a position above the left clavicle. The signal was recorded with a sampling rate of 500 Hz and filtered with a 0.5–40 Hz band-pass filter. In addition, the signal was downsampled to 250 Hz to compare it with the simulated signal. Figs. 4 and 5 also show results from the same subject. The waveform shown in Fig. 4(c) was estimated with Q = 2, and the one shown in Fig. 5 (c) was estimated with Q = 3.

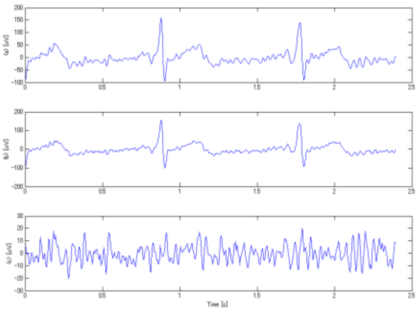

Fig. 4 Results from an actual EEG measurement using an NCR electrode (*Q* = 2). (a) Raw EEG signal obtained using an NCR electrode, (b) estimated ECG component, (c) estimated EEG

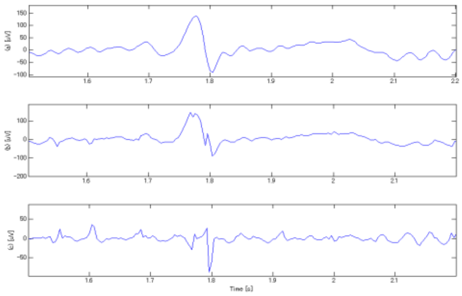

Fig. 5 Results from actual EEG measurements using the NCR electrode (Q = 3). (a) Raw EEG signal using an NCR electrode, (b) estimated ECG component,(c) estimated EEG

C. Evaluation of R wave detection in the EEG signal measured using the NCR electrode

In this study, an evaluation procedure for the separated ECG components was not stated concretely because our previous studies have established that EEG measurement using the NCR electrode produces robust detection of R waves [4, 5, 6]. In our previous studies [4-6], detection rates of R waves in the EEG signal were evaluated. In this paper, we briefly describe the result of R wave detection using datasets identical to those used in our previous studies. In our previous studies, evaluation indices for R wave detection included both sensitivity and specificity, which were determined as sensitivity = (true positive/ true positive + false negative)*100 and specificity = (true positive/true positive + false negative)*100, respectively. As a result, the specificities and sensitivities of the R-wave detection rate ranged from 90%–100%, where the SBR varied from 10–90, indicating the effectiveness of the measurement using the NCR electrode and SNEO-based R-wave detection method.

IV DISCUSSION

In this paper, we propose a method for the separation of a combined EEG and ECG signal to obtain an accurate frequency analysis for the EEG signal and to detect the R wave for the ECG signal using a single EEG measurement. We evaluated this method by using simulated data and evaluated actual signals measured by using an NCR electrode. Fig. 2 illustrates the result produced by the proposed method using simulated data. In Fig. 2(d), a remaining EEG component can be seen within the estimated ECG component. In contrast, Fig. 2(e) shows that the estimated EEG component does not have outstanding QRS complexes and the shape of the estimated EEG component can be approximately reconstructed to resemble the original EEG waveform shown in Fig. 2(a). In addition, Fig. 3 shows that the *INPS* of the alpha, beta1, delta, and theta bands could be accurately contained within the estimated EEG, depending on the parameters used. Moreover, Fig. 2 shows that the suitable neighborhood size was different for each frequency band; for example, the alpha band could be effectively reconstructed when ns = 10 and the delta band was most adequate when ns = 50. These results show that the neighborhood size can, in fact, be selected based on the desired frequency band.

Figs. 4 and 5 show the results from the same actual EEG measurement made using the NCR electrode, implying that the difference between Fig. 4(c) and Fig. 5(c) can be attributed to the value of *Q*. These results demonstrate that the EEG component can be reconstructed by the two smallest eigenvectors, because, as shown in Fig. 5(c), an outstanding spike artifact near the QRS complex was observed in the estimated EEG component at around 1.8 s. In other words, the principle component of the ECG is mainly exists in $Q \geq 3$.

In [4], *INPS* ranged from approximately 0.5 to 1, which is comparable to the accuracy observed in this study. However, in this case, the parameters (e.g., d, R) were not optimized. Therefore, there remains potential for improvement in the proposed method, although this study successfully demonstrated that nonlinear state-space projection is a feasible method to separate simultaneously measured EEG and ECG signal components. In addition, nonlinear state-space projection can be applied to every sample, which is a feature effective for real-time analysis.

V CONCLUSIONS

We reported and evaluated an algorithm for separating EEG and ECG components from a combined EEG-ECG signal recorded using the NCR electrode. The method guarantees accurate detection of R waves in the EEG measurement, which was confirmed by the sensitivity and specificity values of R wave detection of 100% in most SBRs. The proposed separation algorithm was based on nonlinear state-space projection, consisting of the principle component analysis of the phase space of a dynamical system. The evaluation using simulated data showed that the *INPS* of the alpha, beta1, and theta bands of the EEG could be accurately contained within the estimated EEG when SBR = 10 and *Q* = 2. The suitable neighborhood size was different for each frequency band, implying the selected neighborhood size can be optimized for obtaining a desired frequency band of the EEG signal. These results demonstrate the feasibility of nonlinear state-space projection-based separation of EEG and ECG component from combined signals.

REFERENCES

[1] C. Lin, L. Ko, I. Chung, T. Huang, Y. Chen, T. Jung, and S. Liang, “Adaptive EEG-Based Alertness Estimation System by Using ICA-Based Fuzzy Neural Networks,” IEEE Transactions On Circuits And Systems—I: Regular Papers, vol. 53, no. 11, pp. 2469–2476, 2006.

[2] E. A. Schmidt, W. E. Kincses, M. Schrauf, S. Haufe, R. Schubert, and G. Curio, “Assessing Drivers’ Vigilance State During Monotonous Driving,” Proceedings of the Fourth International Driving Symposium on Human Factors in Driver Assessment, Training and Vehicle Design, 2007.

[3] G. Dirlich, L. Vogl, M. Plaschke, and F. Strian, “Cardiac Field Effects on the EEG,” Electroencephalography and Clinical Neurophysiology, vol. 102, pp. 307–315, 1997.

[4] M. Sakai and D. Wei, “Wavelet Shrinkage Applications of EEG-ECG-based Human-computer Interface,” Proceedings of 2008 IEEE 8th International Conference on Computer and Information Technology, pp. 538–543, 2008.

[5] M. Sakai and D. Wei, “Separation of electrocardiographic and encephalographic components based on signal averaging and wavelet shrinkage techniques,” Computers in Biology and Medicine, vol. 39, no. 7, pp. 620–629, Jul. 2009.

[6] M. Sakai, Y. Okuyama, and D. Wei, “Separation of EEG and ECG Components Based on Wavelet Shrinkage and Variable Cosine Window,” Journal of Medical Engineering & Technology, vol. 36, no. 2, pp. 135 –143, 2012.

[7] X. Hu and Nenov, “A single-lead ECG enhancement algorithm using a regularized data-driven filter,” IEEE Trans. BioMed. Eng., vol. 53, pp. 347–351, Feb. 2006.

[8] T. Schreiber and D. T. Kaplan, “Nonlinear Noise Reduction for Electrocardiograms,” CHAOS, vol. 6, pp. 87–92, 1996.

[9] M. Richter, T. Schreiber, and D. T. Kaplan, “Fetal ECG extraction with nonlinear state space projections,” IEEE Trans. Biomed. Eng., vol. 45, no. 1, pp. 133–137, 1998.

[10] H. Park, D. Jeong, and K. Park, “Automated Detection and Elimination of Periodic ECG Artifacts in EEG Using the Energy Interval Histogram Method,” IEEE Trans. Biomed. Eng., vol. 49, no. 12, pp. 1526–1533, 2002.

[11] S. Shahid, G. Prasad, and R. K. Sinha, “On fusion of heart and brain signals for hybrid BCI,” 5th Int. IEEE EMBS Conference on Neural Engineering, Cancun, Mexico. IEEE. pp. 48–52, 2011.

Motoki Sakai received B.E., M.E. and Ph.D. degrees from the university of Aizu, Aizuwakamatsu city, in 2003, 2005 and 2009. He joined QRS Corporation in 2009. He has been a project research associate in Fukushima University Graduate School of Symbiotic Systems Science and Technology since 2010. His current research interests include a biomedical engineering.

Yuichi Okuyama received his M.E. and Ph.D. degrees in computer science and engineering from the University of Aizu in 1999 and 2002, respectively. He joined NTT Corp. in 2002, where he was involved in the design of an application for dynamically reconfigurable hardware. He is currently an assistant professor in the School of Computer Science and Engineering, the University of Aizu. His research interests include image and signal processing, machine learning, and hardware design for image and signal processing. He is a member of IPSJ.

Toshihiro Sato received B.E from the University of Aizu in 2012 and has joined in Dr. Okuyama research team as a master student from April 2012. His research field is the hardware development for signal processing algorithm.

Daming Wei had been a professor and director of Biomedical Information Technology Laboratory, University of Aizu, Japan since April 1999. He is now professor emeritus (life title) of University of Aizu, visiting professor in the Tohoku University Graduate School of Medicine, Sendai, Japan and distinguished “Ziqian” professor in Shanghai University. Prof. Wei has long research history in electrophysiological heart model (known as Wei-Harumi model in some literature) and computer simulation of electrocardiogram. He authors more than 200 scientific papers in scientific journals or major conference proceedings, and 10 books or book chapters in English or Japanese. He is the inventor of 18 patents registered in US, Japan and China, regarding to clinical electrocardiogram.